J|A|C|S COMMUNICATIONS

Published on Web 08/06/2010

Layer-by-Layer Synthesis of Metal-Containing Conducting Polymers: Caged Metal Centers for Interlayer Charge Transport

Wenjun Liu,[†] Weijie Huang,[‡] Maren Pink,[†] and Dongwhan Lee*,[†]

Department of Chemistry, Indiana University, 800 East Kirkwood Avenue, Bloomington, Indiana 47405 and Carl Zeiss SMT Inc., One Corporation Way, Peabody, Massachusetts 01960

Received May 11, 2010; E-mail: dongwhan@indiana.edu

Abstract: Metal-templated [2 + 3]-type cocondensation of a π-extended boronic acid and nioxime furnished a series of cage molecules, which were electropolymerized to prepare metal-containing conducting polymers (MCPs). Despite sharing essentially isostructural organic scaffolds, these materials display metal-dependent electrochemical properties as evidenced by different redox windows observed for M = Co, Fe, Ru. Consecutive electropolymerization using two different monomers furnished bilayer MCPs having different metals in each layer. In addition to functioning as heavy atom markers in cross-sectional analysis by FIB and EDX, redox-active metal centers participate in voltage-dependent interlayer electron transport to give rise to cyclic voltammograms that are distinctively different from those of each layer alone or random copolymers. A simple electrochemical technique can thus be used as a straightforward diagnostic tool to investigate the structural ordering of electrically conductive layered materials.

The development of electronic devices such as light-emitting diodes (LEDs), field-effect transistors (FETs), and photovoltaic cells (PCs) with high efficiency requires the control of molecular organization and orientation at the microscopic level.[1−4] Layered structures built on solid substrates represent one such device architecture.[4−6] With conjugated polymers, multilayer structures are typically prepared by a sequential Langmuir−Blodgett (LB) method[7] or layer-by-layer (LBL) deposition from solution samples.[8] Alternatively, monomeric precursors can be electropolymerized onto the electrode surface, and the polymer-modified electrode can be used as a working electrode to grow a second layer of electroactive material.[9] Under ideal conditions, this process can be repeated to prepare multilayer structures for the directional flow of charge carriers.

Despite a few proof-of-principle examples in the literature to demonstrate the preparation of layered conducting polymer (CP) structures by sequential electropolymerization,[9] direct experimental evidence to confirm the formation of genuine layered structures is hard to attain. This is in part because of the similar elemental compositions of organic CPs comprising each layer. In this communication, we report consecutive electropolymerization of isostructural transition metal complexes to construct electrically conductive bilayer materials. In addition to functioning as heavy atom markers in cross-sectional analysis, caged metal complexes participate in vectorial charge transport across the CP layers to give rise to characteristic cyclic voltammograms (CVs). We demonstrate that a simple electrochemical technique can thus be used as a straightforward and powerful diagnostic tool to distinguish ordered bilayer polymer structures from random copolymer assemblies.

Scheme 1. Polymers Built with Boronic Acid Derived Cage Monomers

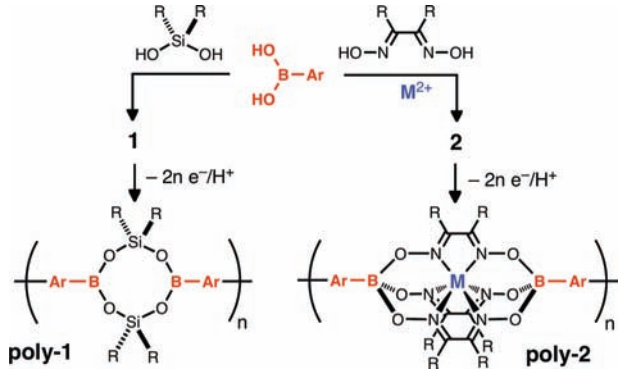

A formal [2 + 2]-type cocondensation reaction between π-extended boronic acids and dihydroxysilanes furnishes borasiloxane cage molecule **1** that can readily be electropolymerized to **poly-1** (Scheme 1).[10,11] As a logical extension of this chemistry, we considered a formal [3 + 2]-type cocondensation between *N*,*N*-bidentate dioximate ligands and π-extended boronic acids. As shown in Scheme 1, this metal-templated assembly should facilitate access to bifunctional monomer **2** from simple and readily modifiable structural subcomponents. Notably, the cage complex **2** supports coordinatively saturated metal ions that are ideal for electron transfer (ET) with minimal structural reorganization.[12] Metal ions encapsulated by this classical macrobicyclic ligand motif have been studied extensively, but no examples are found for their use as CP monomers.[13,14]

The reaction between nioxime (= 1,2-cyclohexane-dione dioxime) and bithiopheneboronic acid in MeOH proceeded in the

Scheme 2. Cage Synthesis and Electropolymerization

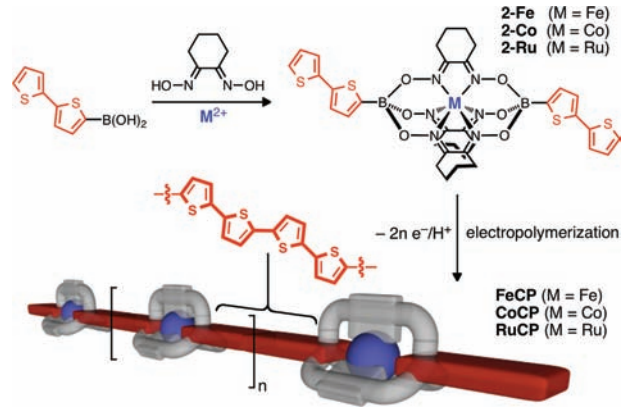

[†] Indiana University.
[‡] Carl Zeiss SMT, Inc.

10.1021/ja104038s

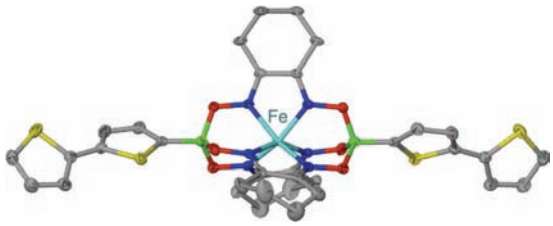

Figure 1. ORTEP diagram of **2-Fe** with thermal ellipsoids at 50% probability.

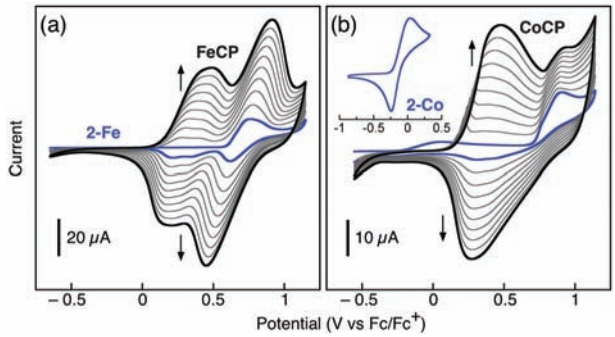

Figure 2. Electropolymerization of (a) **2-Fe** and (b) **2-Co** (inset: CV of **2-Co** monomer within a narrow potential window to isolate metal-based redox process) on Pt button electrodes in CH_2Cl_2 with n-Bu_4NPF_6 (0.1 M) as supporting electrolyte. Scan rate =100 mV/s. T = 298 K.

presence of divalent metal template M^{2+} (= Fe^{2+}, Co^{2+}, Ru^{2+}) to furnish neutral complexes **2-Co**, **2-Fe**, and **2-Ru**, which precipitated from the reaction mixture (Scheme 2). The simple and well-resolved ^{1}H NMR spectral patterns of **2-Fe** and **2-Ru** suggested a low-spin d^6 system with a highly symmetric ligand environment, the structure of which was unambiguously confirmed by single crystal X-ray crystallography (Figure 1). Compound **2-Co** displaying paramagnetically shifted proton resonances was also structurally characterized (Figure S1).

In CH_2Cl_2, **2-Fe** and **2-Ru** display broad oxidative waves at ca. 0.76 and 0.81 V,[15] respectively (Figures 2 and S2). These features arise from the reversible M^{II}/M^{III} couple, which is overlaid with irreversible oxidation (and subsequent homocoupling) of the ligand bithienyl groups. In support of this notion, a reversible redox wave at $E_{1/2}^{ox}$ (Fe^{II}/Fe^{III}) = 0.62 V was displayed by a model complex that shares the identical ligand scaffold with **2-Fe** but has phenyl instead of bithienyl capping groups (Figure S3). For **2-Co**, however, the metal-based and ligand-based redox processes are well resolved to produce a quasi-reversible oxidation wave at $E_{1/2}^{ox}$ = −0.10 V for the Co^{II}/Co^{III} couple (Figure 2b; inset) and a broad ligand-based oxidation at around +0.91 V.

Repetitive voltage sweeps of **2-M** (M = Fe, Co, Ru) in the potential window between −0.4 and +1.4 V (vs Ag/Ag^+) resulted in the deposition of thin film materials on the Pt electrode surface (Figures 2 and S2). Cyclic voltammetry (CV) studies on polymer-modified electrodes in monomer-free electrolyte solutions established the linear dependence of the peak current on the scan rate (Figures S4−S6), which confirmed that the redox activities arise from surface-bound materials. Notably, distinctively different CV patterns observed for a homologous set of systems demonstrate the active functional role played by the metal center in electron shuttling across essentially isostructural scaffolds.

The UV−vis spectra of the polymer film prepared from **2-Fe** (Figure S7) showed development of longer-wavelength transitions upon oxidation, which reflects the evolution of polaronic/bipolaronic states along the π-conjugated polymer backbone (Scheme 2).[10] The

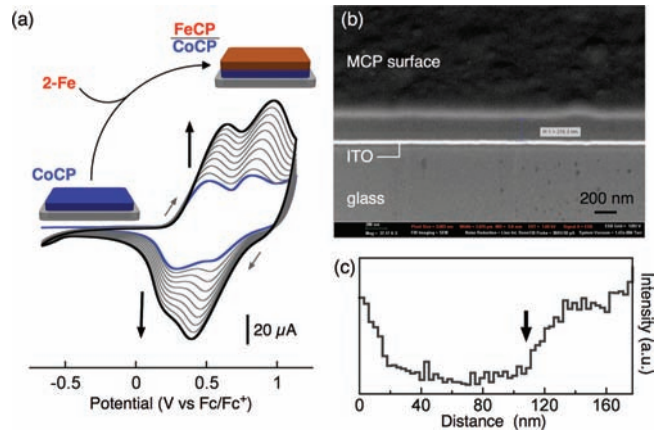

Figure 3. (a) Electropolymerization of **2-Fe** onto **CoCP** layer on a Pt electrode. (b) Cross-sectional FESEM image of **CoCP**−**FeCP** bilayer on ITO-coated glass milled by FIB. (c) Pixel-average profile of the **CoCP**−**FeCP** bilayer generated by measuring the FESEM signal intensity and averaging 300 pixels along a direction perpendicular to the electrode surface from top to bottom, with x = 0 corresponding to the top surface of the material. The arrow indicates the location of discontinuity in the signal intensity.

formation of a densely packed layer of metal-containing conducting polymer (MCP) was subsequently confirmed by field emission SEM (FESEM) and cross-sectional analysis of the thin film using focused ion beam (FIB) milling (Figure S8). The elemental composition of this material was also probed using energy dispersive X-ray analysis (EDX), which confirmed the presence of Fe and S in addition to other elements (Figure S9).

With preliminary results obtained for the growth of MCPs on the electrode surface, we proceeded to prepare bilayer structures using sequential electropolymerization. We anticipated that a layer of electrically conductive MCP deposited onto ITO would effectively function as a working electrode for subsequent growth of the second layer of MCP using different monomers. Under a standard anodic voltage sweep (see Figure 2), the cobalt cage complex **2-Co** was polymerized to prepare a **CoCP** (= poly(**2-Co**))-modified ITO electrode, which was placed in an electrolyte containing either the iron-containing monomer **2-Fe** (Figure 3) or ruthenium-containing monomer **2-Ru** for a second round of anodic polymerization.

The atomic compositions of these bilayer materials were probed by EDX analysis, which confirmed the presence of cobalt and iron for **CoCP**−**FeCP** (Figure S10a) and cobalt and ruthenium for **CoCP**−**RuCP** (Figure S10b). A close inspection of the FESEM image of the **CoCP**−**FeCP** sample milled by FIB (Figure 3b) revealed a discontinuity at the layer-to-layer interface (Figure S11). Such a feature does not exist in the "homopolymer" bilayer sample **CoCP**−**CoCP** comprised of two compositionally identical layers (Figure S12).[16] A more quantitative analysis of this bilayer feature was aided by the pixel-average profile analysis. As shown in Figure 3c, the discontinuity in the FESEM signal intensity was located at about 110 nm from the top surface of the **CoCP**−**FeCP** (overall thickness = ca. 220 nm). A similar result was obtained for the **CoCP**−**RuCP** bilayer (Figure S13).

With densely packed MCP bilayers assembled on the electrode surface, we investigated electron transport across their interface. As shown in Figure 4,[17] the CV of **CoCP**−**FeCP** displays two broad redox waves that are centered at E_1^{ox} = 0.40 and E_2^{ox} = +0.67 V. Notably, the onset oxidation potential of **CoCP**−**FeCP** at +0.17 V is identical to that (+0.17 V) of **CoCP**, despite the fact that **FeCP** can be oxidized at a significantly lower onset potential of +0.06 V.

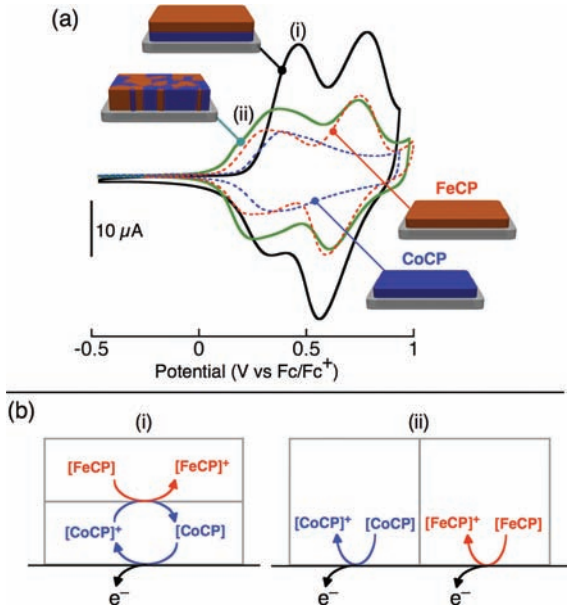

Figure 4. (a) CVs of (i) **CoCP**−**FeCP** bilayer (black solid line) and (ii) random copolymer of **(Co/Fe)CP** (green solid line) on Pt electrodes in CH_2Cl_2 with n-Bu_4NPF_6 (0.1 M) as supporting electrolyte. CVs of FeCP (red dotted lines) and CoCP (blue dotted lines) measured under similar conditions are overlaid for comparison (scan rate = 25 mV/s; T = 298 K). (b) Schematic representations of interfacial ET processes in (i) and (ii).

This observation is consistent with the sequential electron transfer model depicted in Figure 4b. Here, the oxidation of the top layer (**FeCP**), despite having a lower onset potential, cannot occur until oxidation of the bottom layer (**CoCP**) generates a sufficient amount of charge carriers through anodic doping. The **CoCP** layer thus functions as a redox mediator for ET from the electrode surface to **FeCP**, and its continuous regeneration gives rise to a significant enhancement in the faradaic current compared with that of the **CoCP** layer alone. With an increase in doping level with the anodic potential sweep, the Fe^{II}/Fe^{III} redox couple of the **FeCP** layer dominates the CV feature of **CoCP**−**FeCP** at $E_2^{ox} = +0.67$ V, which is absent in the **CoCP**-only sample (Figure 4a).

The electrochemical consequence of the layered structural organization is evident from comparative studies with the random copolymer (**Co/Fe)CP** (Figure 4), prepared by electropolymerization of an equimolar mixture of **2-Co** and **2-Fe**. As shown in Figure 4a, the CV of this material is essentially identical to the sum of the individual signals from the **CoCP** and **FeCP** components since the redox process of the latter does not rely on that of the former in the random copolymer environment (Figure 4b). A similar electrochemical behavior was observed for bilayer **CoCP**−**RuCP** vs random copolymer (**Co/Ru)CP** (Figure S14). The use of isostructural monomers in bilayer construction ensures that the overall internal structure remains essentially invariant from layer to layer. Therefore, the migration/permeation of counterions into the film during the redox process should not be the discriminating factor responsible for the markedly different experimental observations made for the layer-by-layer vs random copolymer composites.

An intimate interplay between metal-based and polymer-based redox processes has been studied extensively using MCPs that are typically built with metallocenes or square-planar coordination complexes of multidentate ligands.[18] We have now shown that classical tris(dioximate) cages can be used as a robust structural platform to support π-conjugated organic fragments across the metal center. Sequential redox processes mediated by these hybrid materials give rise to characteristic electrochemical signatures that can be utilized as a simple but powerful diagnostic tool to confirm the formation of genuine bilayer CP structures.

Acknowledgment. This work was supported by the U.S. Army Research Office (W911NF-07-1-0533) and the National Science Foundation (CAREER CHE 0547251). D.L. is an Alfred P. Sloan Research Fellow.

Supporting Information Available: Synthesis, characterization, additional electrochemical data, and crystallographic data. This material is available free of charge via the Internet at http://pubs.acs.org.

References

(1) *Organic Electronics*; Klauk, H., Ed.; Wiley-VCH: Weinheim, 2006.
(2) Thematic issue on organic electronics and optoelectronics: *Chem. Rev.* **2007**, *107*, 923−1386.
(3) (a) Venkataraman, D.; Yurt, S.; Venkatraman, B. H.; Gavvalapalli, N. *J. Phys. Chem. Lett.* **2010**, *1*, 947–958. (b) Special issue on organic photovoltaics: *Acc. Chem. Res.* **2009**, *42*, 1689−1857.
(4) Yang, F.; Shtein, M.; Forrest, S. R. *Nat. Mater.* **2005**, *4*, 37–41.
(5) Granstrom, M.; Petritsch, K.; Arias, A. C.; Lux, A.; Andersson, M. R.; Friend, R. H. *Nature* **1998**, *395*, 257–260.
(6) Zotti, G.; Vercelli, B.; Berlin, A. *Acc. Chem. Res.* **2008**, *41*, 1098–1109.
(7) (a) Kim, J.; McQuade, D. T.; Rose, A.; Zhu, Z.; Swager, T. M. *J. Am. Chem. Soc.* **2001**, *123*, 11488–11489. (b) Matsui, J.; Sato, Y.; Mikayama, T.; Miyashita, T. *Langmuir* **2007**, *23*, 8602–8606.
(8) Decher, G. *Science* **1997**, *277*, 1232–1237.
(9) (a) Thompson, L. A.; Kowalik, J.; Josowicz, M.; Janata, J. *J. Am. Chem. Soc.* **2002**, *125*, 324–325. (b) Hao, Q.; Wang, X.; Lu, L.; Yang, X.; Mirsky, V. M. *Macromol. Rapid Commun.* **2005**, *26*, 1099–1103. (c) Hwang, E.; de Silva, K. M. N.; Seevers, C. B.; Li, J.-R.; Garno, J. C.; Nesterov, E. E. *Langmuir* **2008**, *24*, 9700–9706.
(10) Liu, W.; Pink, M.; Lee, D. *J. Am. Chem. Soc.* **2009**, *131*, 8703–8707.
(11) For recent reviews on boronic acid derived functional materials, see: (a) Severin, K. *Dalton Trans.* **2009**, 5254–5264. (b) Korich, A. L.; Iovine, P. M. *Dalton Trans.* **2010**, *39*, 1423–1431.
(12) A conceptual linkage can be drawn to magnetic interactions between two metal centers across the tris(dioximato)metalate(II) "bridge". See: Birkelbach, F.; Florke, U.; Haupt, H.-J.; Butzlaff, C.; Trautwein, A. X.; Wieghardt, K.; Chaudhuri, P. *Inorg. Chem.* **1998**, *37*, 2000–2008.
(13) Voloshin, Y. Z.; Kostromina, N. A.; Krämer, R. *Clathrochelates: Synthesis, Structure and Properties*; Elsevier: Amsterdam, 2002.
(14) (a) Voloshin, Y. Z.; Varzatskii, O. A.; Vorontsov, I. I.; Antipin, M. Y.; Lebedev, A. Y.; Belov, A. S.; Palchik, A. V. *Russ. Chem. Bull., Int. Ed.* **2003**, *52*, 1552–1561. (b) Robbins, M.; Naser, D.; Heiland, J.; Grzybowski, J. *Inorg. Chem.* **1985**, *24*, 3381–3387. (c) Gribble, J.; Wherland, S. *Inorg. Chem.* **1989**, *28*, 2859–2863. (d) Pantani, O.; Naskar, S.; Guillot, R.; Millet, P.; Anxolabéhère-Mallart, E.; Aukauloo, A. *Angew. Chem., Int. Ed.* **2008**, *47*, 9948–9950. (e) Muller, J. G.; Grzybowski, J. J.; Takeuchi, K. J. *Inorg. Chem.* **1986**, *25*, 2665–2667.
(15) Unless noted otherwise, all the potentials are externally referenced to the Fc/Fc^+ redox couple.
(16) When the electrons impinge upon two materials with distinct conductivities, different secondary electron yields result. Although Co and Fe atoms might have similar secondary electron yields, its interaction with the ligand environment could change the electronic properties of each layer, including conductivity. The intensity of the signal depends on the amount of secondary electrons detected and used to construct the FESEM image.
(17) The cartoon-type rendition of **(Co/Fe)CP** here emphasizes no particular structural ordering along the *z*-direction with respect to the electrode surface, which distinguishes this random copolymer from compositionally equivalent bilayer **CoCP-FeCP**.
(18) (a) Stott, T. L.; Wolf, M. O. *Coord. Chem. Rev.* **2003**, *246*, 89–101. (b) Holliday, B. J.; Swager, T. M. *Chem. Commun.* **2005**, 23–36. (c) Wolf, M. O. In *Handbook of Thiophene-Based Materials: Applications in Organic Electronics and Photonics*; Perepichka, I. F., Perepichka, D. F., Eds.; John Wiley & Sons: Chichester, 2009; pp 293−319.

JA104038S